Shock Waves (2005) 14(3): 205–215
DOI 10.1007/s00193-005-0265-6

ORIGINAL ARTICLE

M. Kuznetsov · V. Alekseev · I. Matsukov · S. Dorofeev

DDT in a smooth tube filled with a hydrogen–oxygen mixture

Received: 20 January 2004 / Accepted: 15 December 2004 / Published online: 12 September 2005

Abstract Results of experimental study on DDT in a smooth tube filled with sensitive mixtures having detonation cell size from 1 to 3 orders of magnitude smaller than the tube diameter are presented. Stoichiometric hydrogen–oxygen mixtures were used in the tests with initial pressure ranging from 0.2 to 8 bar. A dependence of the run-up distance to DDT on the initial pressure is studied. This dependence is found to be close to the inverse proportionality. It is suggested that the flow ahead of the flame results in formation of the turbulent boundary layer. This boundary layer controls the scale of turbulent motions in the flow. A simple model to estimate the maximum scale of the turbulent pulsations (boundary layer thickness) at flame positions along the tube is presented. The largest scale of the turbulent motions at the location of the onset of detonation is shown to be 1 order of magnitude greater than the detonation cell widths, λ, in all the tests. It is suggested that the onset of detonation is triggered during flame acceleration as soon as the maximum scale of the turbulent pulsations increases up to about 10λ. The model to estimate the maximum size of turbulent motions, δ, and the correlation $\delta \approx 10\lambda$, give a basis for estimations of the run-up distances to DDT in tubes with internal diameter $D > 20\lambda$.

Keywords DDT · Onset of detonations · Flame acceleration · Run-up distance · Boundary layer

PACS 47.40.-x; 47.27.Nz

This paper was based on work that was presented at the 19th International Colloquium on the Dynamics of Explosions and Reactive Systems, Hakone, Japan, July 27 - August 1, 2003

Communicated by J.E. Shepherd

M. Kuznetsov · S. Dorofeev (✉)
Forschungszentrum Karlsruhe, P.O. Box 3640,
76021 Karlsruhe, Germany
E-mail: sergey.dorofeev@fmglobal.com

V. Alekseev · I. Matsukov
Russian Research Center, Kurchatov Institute, Kurchatov square 1,
123182 Moscow, Russia

1 Introduction

Many practical applications involve handling of extremely sensitive gaseous combustibles in tubes with characteristic sizes, which exceed considerably typical chemical length scales of the mixture, such as detonation cell size, λ. If these mixtures are ignited the combustion process can easily end up with the transition from deflagration to detonation (DDT). In these cases, an important problem to be solved is where can the onset of detonation occur, rather than can it be expected or not. This problem is related to creation of conditions that are necessary for the onset of detonation during the process of flame propagation.

It has been shown by many investigators that a flame should reach high, generally supersonic speed, to create conditions necessary for the onset of detonations [1, 2, 3, 4]. The process of flame acceleration is affected significantly by obstructions along the flame passage [2, 3, 4]. In many situations with dense obstructions, the growth of the flame surface can be the leading factor affecting the rate of flame acceleration [5].

Different physical mechanisms are expected to play their roles in relatively smooth tubes or channels. In particular, flow turbulence generated ahead of the flame due to interactions with tube walls may be important [1]. It has been demonstrated by Schelkin [6] and Soloukhin [7] that flame acceleration and transition to detonation in tubes both are strongly affected by wall roughness. Generation of turbulent boundary layer in the flow ahead of the flame promotes flame acceleration. Moreover, during propagation in a rough/smooth tube the flame shape often turns into a characteristic "tulip" form with the leading edges near the tube walls. It was also reported by Soloukhin [7] that the local explosion, which finally results in the onset of detonation, occurs near the tube wall in regions where the most intense flow–wall interactions take place.

Thus, the processes of flame acceleration and DDT in tubes without obstacles, which are filled with highly sensitive mixtures, differ significantly from DDT in obstructed tubes at nearly critical conditions. Present study addresses

the situation with highly sensitive mixture and relatively smooth tubes. The objective of this work was investigation of DDT process for stoichiometric hydrogen–oxygen mixture. Run-up distances for the onset of detonations were studied in a series of tests as a function of the initial pressure.

There are some experimental data on the effects of tube diameter, initial pressure, and temperature on the run-up distance to detonation, X_D, for tubes without obstacles [8, 9, 10, 11, 12, 13, 14, 15]. These data show a decrease of the run-up distance with initial mixture pressure, p. If such a dependence is expressed in a power form: $X_D \propto p^{-m}$, the exponent, m, depends on mixture properties and lies in the range from 0.4 to 0.8 for various mixtures for the pressure range from 0.1 to 6.5 bar. In particular, data points for mixture $1.5H_2 + O_2$ [14], can be approximated as $X_D \propto p^{-m}$, with $m = 0.76 \pm 0.2$.

In some of these studies, an increase of the run-up distance with tube diameter was reported, Lafitte [9], Bollinger et al. [14, 15]. The ratio of the run-up distance to the tube diameter X_D/D was found to be in the range from 15 to 40. On the contrary, Bollinger et al. [14, 15] noted that only for rich mixtures of hydrogen fuel the run-up distance depends on the tube diameter. Somewhat ambiguous data on the effect of the tube diameter may be due to the hidden influence of other factors, such as tube roughness. It should be noted that no reliable model is presently available to link the run-up distance with parameters of mixture sensitivity (such as the detonation cell size), tube diameter, wall roughness and others. This situation is partially due to the fact that many tests were performed in relatively short tubes. In these cases, mixture pre-compression effects may be important, so it is difficult to describe the mixture properties as that of the initial mixture. Also, as it was found by Salamandra et al. [16], the transition to detonation in short tubes can be facilitated by the flame interaction with the reflected pressure waves. In addition, the tube roughness, which plays a role [6, 7], was not always sufficiently characterized.

2 Experimental

Experiments were performed in a smooth detonation tube of 105-mm inner diameter (wall thickness was 4.5 mm) and 24-m length. The relatively large length of the tube (the ratio of tube length to tube diameter, L/D, was equal to 230) provided conditions to reduce possible effects of the end-wall reflections and global pre-compression on DDT processes. Schematic sketch of the facility is shown in Fig. 1. The tube was made of a steel pipe and consisted of four sections smoothly welded with each other. The roughness of the internal tube walls was 50 μm as specified by the tube manufacturer. The tube was equipped with 24 measuring ports located at cylindrical surface and three ports at the ignition end (axial one was for the ignition plug, and two parallel were for photo-gauges). Tube was located horizontally with small tilt to provide water drainage after each test.

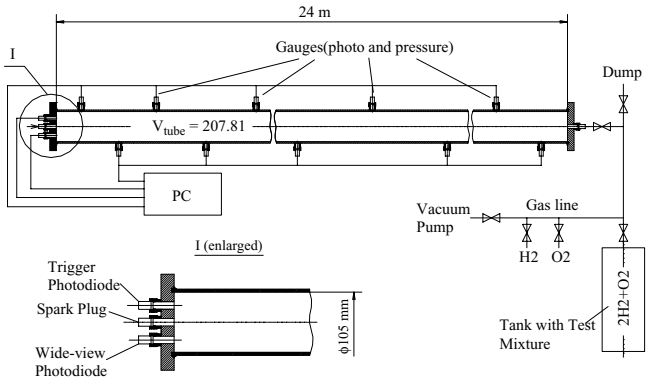

Fig. 1 Scheme of experimental facility

Stoichiometric H_2–O_2 mixture at initial pressures from 0.2 to 8 bar was used in the tests. Detonation cell sizes of these mixtures vary from 8.5 mm (0.2 bar) to 0.17 mm (8 bar) [17, 18]. This means that $D \gg \lambda$, and DDT can easily occur in 105-mm tube.

A glow plug was used for ignition to avoid possible direct initiation of detonations by a spark plug. Collimated germanium photodiodes FD-9 and FD-10 were used to record flame front times-of-arrival and light intensity signals. One of the photodiodes was installed in the tube axially to record light signal from the combustion process continuously. With this gauge it was possible to define the time of the onset of detonation by specific inflection of the signal curve. Two types of pressure transducers were used to record pressures. These were piezoelectric transducers PCB-H113A and piezoresistive transducers D6 (R&D Institute "Teplopribor", Moscow, Russia). Both the pressure transducers and the photodiodes were flush-mounted in the tube wall to minimize the flow disturbance. The effective roughness related to the instrument ports, if weighted by the respective surface areas, was much smaller than the original tube roughness of 50 μm. The locations for the onset of detonations in the tests were not correlated with the locations of the instrument ports.

3 Properties of test mixtures

Detonation parameters and flame properties of the test mixtures were calculated for the following data analysis. These data are presented in Table 1. Thermodynamic parameters were calculated using STANJAN code [19]. Laminar burning velocities and flame thickness were calculated using FP code [20] with check of some control points given by experimental data of Koroll et al. [21]. Experimental values of the detonation cell sizes measured by Manzhalei et al. [17] are presented in Table 1. A comparison of the experimental data and the cell sizes calculated using model of Gavrikov et al. [18] is presented in Fig. 2. The agreement within a factor of 2 is observed between the experimental and calculated cell sizes. This should be considered as a good agreement

Table 1 Flame properties and detonation parameters of test mixtures

Initial pressure (p, bar)	Adiabatic complete combustion pressure (P_{icc}, bar)	Expansion ratio (σ)	Sonic velocity in products (c_p, m/s)	Laminar burning velocity (S_L, m/s)	Laminar flame thickness (δ_T, mm)	Chapman–Jouguet velocity (D_{CJ}, m/s)	Chapman–Jouguet pressure (P_{CJ}, bar)	Detonation cell size (λ, mm)
0.2	1.9	8.10	1,350	7.1	0.35	2,760	3.7	8.52
0.3	2.9	8.20	1,360	8.4	0.2	2,780	5.6	5.54
0.5	4.8	8.33	1,370	9.2	0.11	2,800	9.5	3.23
0.8	7.9	8.44	1,380	10.2	0.066	2,830	15	1.96
1	10	8.50	1,380	10.6	0.051	2,840	19	1.55
2	20	8.68	1,400	11.6	0.024	2,880	40	0.74
3	31	8.78	1,410	12.2	0.016	2,900	61	0.48
4	42	8.86	1,420	12.2	0.012	2,920	82	0.36
5	52	8.92	1,420	12.2	0.01	2,930	103	0.28
6	63	8.96	1,430	12.3	0.008	2,940	124	0.23
8	85	9.04	1,430	12.2	0.006	2,960	167	0.17

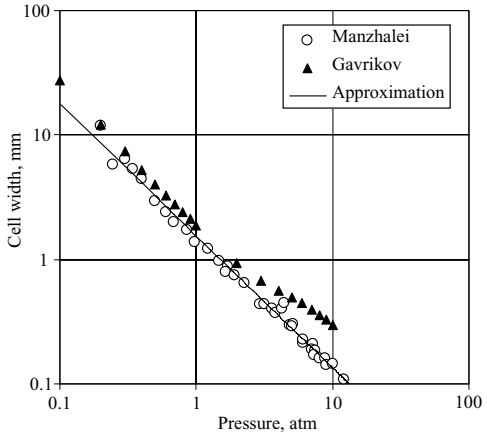

Fig. 2 Detonation cell size as a function of initial pressure

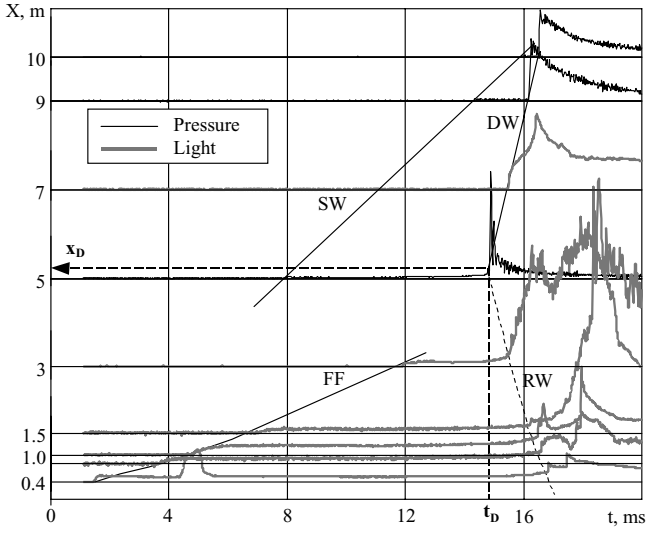

Fig. 3 X–t diagram of explosion processes for 0.2 bar initial pressure (data for initial 10 m are shown). *FF*, flame front trajectory; *SW*, lead shock trajectory; *DW*, detonation front trajectory; *RW*, retonation wave

for the detonation cell sizes, because the accuracy of the experimental values is usually estimated by a factor of 2, and the same accuracy is suggested for the model by Gavrikov et al. [18].

It is interesting to notice that the laminar burning velocities and sound speeds are very similar in all the mixtures tested. The sound speed in reactants c_r is 530 m/s independent of the initial pressure. The speed of sound in products c_p varies in the range from 1,350 to 1,430 m/s. The laminar burning velocity varies from about 7 to 12 m/s. The expansion ratio (ratio of densities between reactants and products) is also almost constant, so that the initial visible flame velocity is estimated to be in the range from 60 to 110 m/s for all the initial pressures. The detonation velocity changes only slightly with pressure. The detonation cell size, however, decreases by 2 orders of magnitude with the initial pressure increase from 0.2 to 8 bar. The same is true for the laminar flame thickness.

4 Results

In the tests over all the range of the initial pressures, ignition was followed by flame acceleration and then the onset of detonation was observed. Characteristic X–t diagram of the explosion process is shown in Fig. 3. This diagram shows records of the pressure transducers and photodiodes as well as the trajectories of the flame, shock, detonation, and retonation waves. It is seen that detonation occurs at about 5 m from the ignition point in this particular test. Pressure records show a compression wave ahead of the flame. The head of the compression wave typically formed a shock. The overpressures recorded in the lead shocks were about 1.4 of the initial pressure, p, for tests with p from 0.2 to 1 bar (the compression waves ahead of the flame were not resolved in tests with $p > 1$ bar, because of short run-up distances). The Mach numbers of the lead shocks were about 1.5. Detonations occurred significantly behind the lead shock in a region close to the flame as it is seen in Fig. 3. We should note once more that such a good spatial resolution of all the waves in X–t diagram was only achievable for relatively low initial pressures.

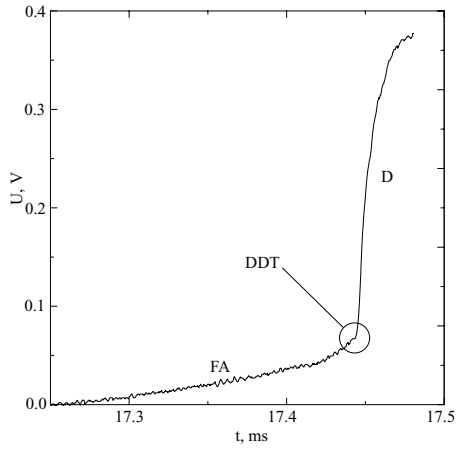

Fig. 4 Typical record from "DDT" photodiode. *FA*, flame acceleration; *D*, detonation; *DDT*, DDT point

Due to the finite number of the photodiodes and pressure transducers it is difficult to define precisely the location of the onset of detonation along the tube just from the data of X–t diagrams. To improve accuracy of determination of the run-up distances to DDT, an additional wide-view photodiode was used, which was mounted at the ignition end of the tube. A typical signal of such a photodiode is shown in Fig. 4. The light intensity recorded by the photodiode increases sharply at the time of the onset of detonation. Such records permitted to define precisely the time of the detonation onset, t_D. Knowing the value of t_D, it is easy to define the DDT run-up distance, X_D, from X–t diagrams using the intersection of the detonation trajectory with the vertical line at t_D, as shown in Fig. 3. This procedure allowed us to determine the run-up distance even in the tests when the onset of detonation was observed prior to the first measuring station.

Dependencies of the flame velocities on distance for initial pressures of 0.3, 0.5, 1, and 8 bar are shown in Fig. 5. The velocities were determined from the arrival times of a pair of the photodiodes and the value was attributed to the location of the second one from each pair. It is seen that the flame velocities (respective to fixed observer) reached a value of about 800 m/s before the transition to detonation for all the tests. At the transition location, the detonation speed was considerably overdriven (up to 4,000 m/s) dropping then down to the Chapman–Jouguet (CJ) values, which were from 2,760 to 2,960 m/s. Detonation speeds and overpressures approached CJ values in about 1 m from the transition location.

A comparison between calculated and experimentally defined detonation velocities is shown in Fig. 6. It is seen that the experimental and theoretical values agree within the relative accuracy of ±3%. This indicates that detonations were steady state and propagated without noticeable losses. Experimental data on the maximum detonation pressures are shown in Fig. 7 in comparison with calculated CJ values. There is a good agreement between measured and calculated pressures, suggesting that the von-Neumann spike was not resolved in the tests, as follows from spatial and temporal resolutions available.

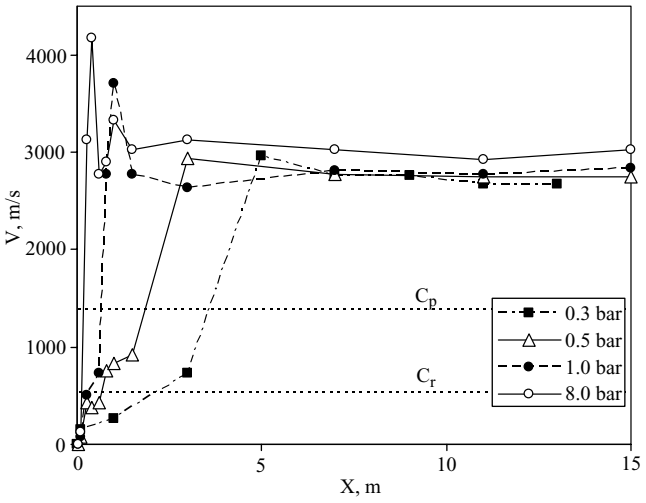

Fig. 5 Dependence of flame velocity vs. distance at different initial pressures

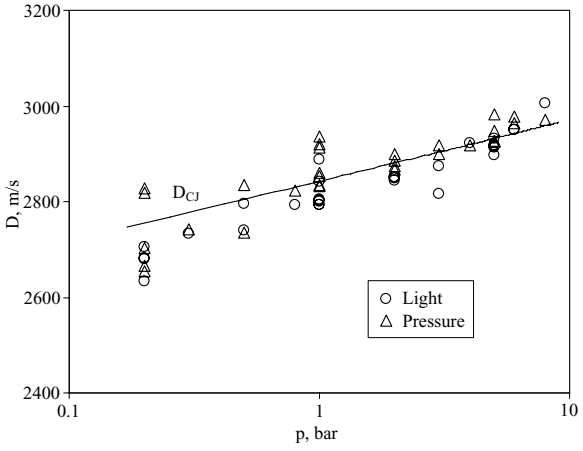

Fig. 6 Comparison of detonation velocities with CJ values

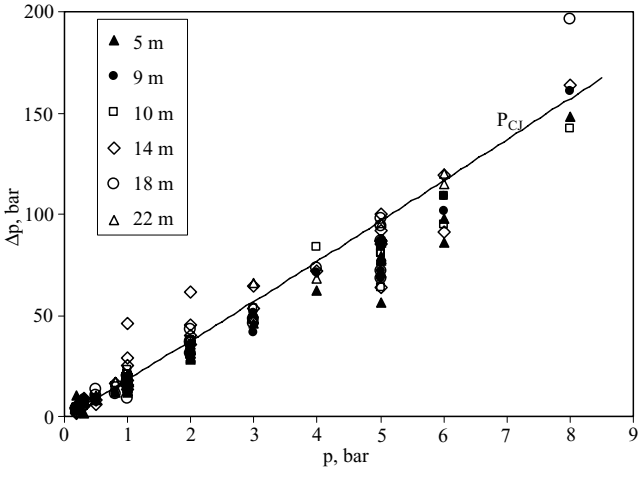

Fig. 7 Comparison of the maximum detonation overpressures with CJ values

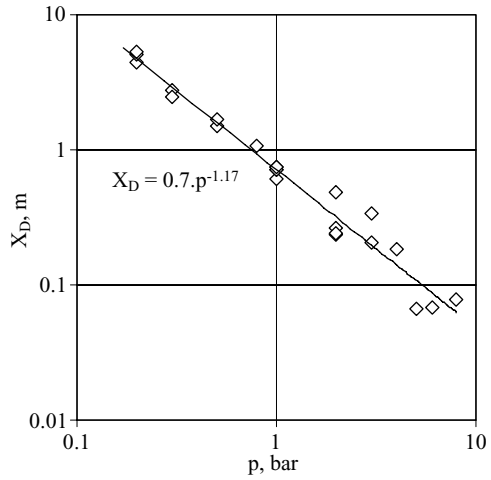

Fig. 8 Run-up distance to DDT vs. initial pressure

The distance from the ignition point to the transition location X_D was found to decrease with initial pressure (see Fig. 8). The dependence of this run-up distance on initial pressure was found to be close to inverse proportionality: $X_{\mathrm{D}} = (0.7 \pm 0.04)p^{-(1.17\pm0.05)}$, where uncertainties were defined by the standard regression analysis. For the highest initial pressures, the run-up distances were as small as one tube diameter. Although the run-up distances were determined with a high accuracy in each particular test (relative systematic error was ±2.5%), different values were obtained in repeated tests. Generally, the scatter of data increased with the increase of the initial pressure. The run-up distances for the same initial pressure differed from the average values by less than 10% for initial pressures from 0.2 to 1 bar, and by up to 50% for initial pressures of 2 and 3 bar.

The pressure dependence of the run-up distance with exponent $m = -1.17 \pm 0.05$ in the present tests was found to be stronger than that for mixture of $1.5H_2 + O_2$ [14] with $m = -0.76 \pm 0.2$. This difference can be attributed both to different mixture properties and to different tubes used. Generally, there are no arguments that pressure dependence of the run-up distances can be considered as a universal function.

5 Discussion

5.1 Role of mixture sensitivity parameters

It has been shown by many investigators that critical conditions for DDT depend on parameters of mixture sensitivity such as the detonation cell size. The minimum tube diameter for DDT to be possible, e.g., should exceed the detonation cell width λ [3]. The minimum size of a detonation kernel, a region of mixture close to self-ignition (or so-called hot spot) that is able to trigger detonation through SWACER mechanism (Shock Wave Amplification by Coherent Energy Release) [22, 23], was estimated to be of the order of 10λ [24, 25, 26]. In the present tests, the detonation cell sizes were very small compared to the tube diameter. This means that there were practically no scale limitations on the possibility of the onset of detonation. The run-up distance was naturally decreasing with increase of the mixture sensitivity (decrease of λ). Because both, the run-up distance and the cell size are nearly inversely proportional to the initial pressure, it can be easily found that the run-up distance appeared to be proportional to the cell size:

$$X_D \approx 550\lambda. \quad (1)$$

This relation, however, does not have any generality except of the obvious decrease of the run-up distance with mixture sensitivity. It cannot be used to estimate the run-up distances in different tubes or mixtures. Indeed, the run-up distance does not characterize directly a possible size of the pre-conditioned mixture that can lead to detonation formation. It does not correspond to any characteristic nonuniformity size in the flow either. It might be possibly linked to other parameters that are more relevant for the onset of detonation. Such a link will be a subject of the following discussion.

For the very sensitive mixtures used in the present tests, the onset of detonation should easily occur once the necessary mixture pre-conditioning is achieved. In this sense, the run-up distance should be sufficient for the flame to generate conditions, which allow a spontaneous explosion to occur somewhere behind the precursor shock, near the turbulent flame brush. Numerous experimental data indicate that the flame velocity should achieve the value of about 1/2 of the CJ detonation velocity for these conditions to be possibly created. It was indeed observed in the present tests that the flame speed before the onset of detonation reached a value of about 800 m/s. Since the initial flame speed was similar in all the mixtures, the difference in the run-up distances can be related to ability of flames to accelerate from initial speed of about 80 m/s to the speed of about 800 m/s. The rate of flame acceleration should depend on the flame surface evolution and on the local turbulent burning velocity. The latter depends on the ratio of turbulent fluctuation velocity u' and laminar burning velocity S_L and on the turbulent Reynolds number, Re_T. The Reynolds number can be expressed as: $Re_T = (u'/S_L)(L_T/\delta_T)$, where L_{T} is the integral scale of turbulence, and δ_T is the laminar flame thickness. All the tests were in the same tube; characteristic velocities were also the same. Such a very general reasoning shows that the laminar flame thickness, δ_T, is the only parameter, which can be responsible for the difference in the rates of flame acceleration and in characteristic flame acceleration distances. Experimental data show that the run-up distances are proportional to δ_T:

$$X_D \approx 13{,}000\delta_T. \quad (2)$$

Again, this relation between the run-up distances and laminar flame thickness does not have any generality and is valid

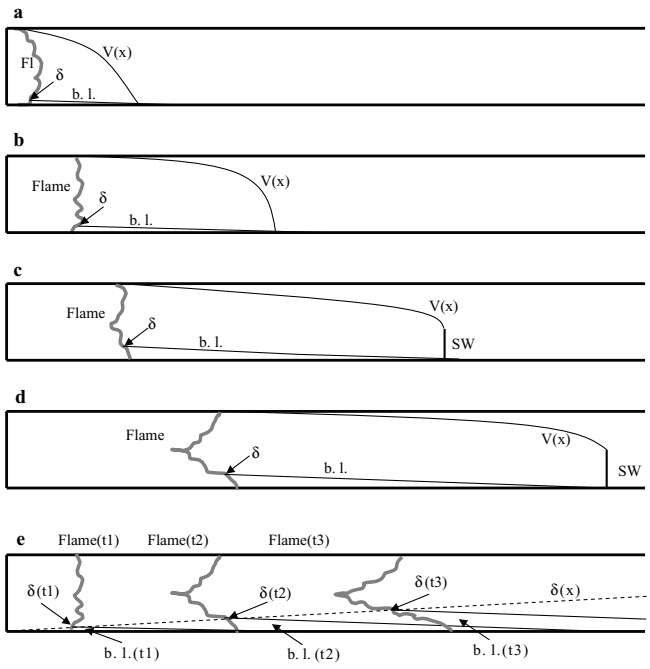

Fig. 9 Sketch showing development of boundary layer ahead of accelerated flame with time (**a**, **b**, **c**, and **d**). Curves $V(x)$ show qualitatively the distribution of flow velocity; *SW*, shock wave; *b.l.*, boundary layer; δ, boundary layer thickness at flame position. **e** shows flame positions and boundary layers at three different moments of time $t1$, $t2$, and $t3$. Curve $\delta(x)$ shows boundary layer thickness at flame positions as a function of distance

only for the present series of tests. Also, flame acceleration to a speed of about 1/2 of the CJ detonation velocity can be considered as necessary, but not as a sufficient condition for DDT.

5.2 Turbulent boundary layer

As it was reported by Schelkin [6] and Soloukhin [7] and other investigators, the tube wall roughness and formation of the turbulent boundary layer are extremely important for the flame acceleration and DDT. For the majority of the present tests (initial pressures from 0.2 to 3 bar) the run-up distances exceeded 5 tube radii and initial, nearly spherical, stage of flame propagation can be assumed to be of relatively minor importance. For these range of initial conditions, Fig. 9 shows qualitatively the evolution of the flow ahead of the accelerated flame. Initially, the flow may have smooth velocity distribution $V(x)$, as shown in Fig. 9a. The maximum flow speed can be estimated as $(\sigma - 1)S_L$, that is about 100 m/s for our tests. The velocity profile is expected to sharpen with time (Fig. 9b) and at some stage a shock should be formed ahead of the flame. Depending on details of the flame acceleration, the shock may be formed at the head of the compression wave, which propagates with the sound speed, c_r, as shown in Fig. 9c, or somewhere closer to the flame. At the same time, the flow's interaction with tube walls results in formation of the turbulent boundary layer [27]. The thickness of the layer grows with time of flow–boundary interactions. The boundary layer starts to appear in the compression wave and continues to grow after the lead shock is formed. At a later stage, a situation shown in Fig. 9d is developed with the lead shock and growing boundary layer behind it. Interactions of the flame with boundary layer results in a significant increase of the burning rate near the tube walls, and a characteristic "tulip" flame shape is formed as reported by Schelkin and Soloukhin.

It is useful to estimate the distances for formation of the shocks ahead of the flame for conditions of the present tests. Such an estimate was made using one-dimensional 'simple wave' theory [27]. Assuming for simplicity that the rate of flame acceleration, a, is constant for each given initial pressure, the time, t_{sh}, and distance, X_{sh}, for formation of the shock can be calculated. The average rate of flame acceleration can be determined from the experimental data. The results of these estimates are presented in Table 2 for three different initial pressures. The flame positions at the time of the shock formation, X_{fl}, and the experimental run-up distance to DDT, X_D, are shown in Table 2 for comparison. Estimates for initial pressure of 8 bar are also included in Table 2. In this case, the shock is formed during initial spherical stage of flame propagation before any reflection of the acoustic waves from the tube walls takes place. We should note that for intermediate cases, which cannot be considered either as spherical or planar, such simple estimates for the shock formation distances could not be provided.

Our estimates show that the shock is formed at a distance of about 1/2 of the run-up distance to DDT. The flame position at the time of the shock formation is roughly in the middle between the shock and the ignition point. Figure 9e shows the flame positions and boundary layers at three different moments of time $t1 < t2 < t3$. While the flame propagates along the tube it interacts with the boundary layer, which becomes thicker and thicker along the flame path. The thickness of the boundary layer grows with time while the flow interacts with the wall. The origin of the boundary layer (the head of the compression wave or the lead

Table 2 Comparison of shock formation distance, flame position and detonation onset distance

Initial pressure (p, bar)	Flame acceleration rate (a, $\times 10^5$ m/s^2)	Shock formation time (t_{sh}, ms)	Flame position at shock formation (X_{fl}, m)	Shock formation distance (X_{sh}, m)	Experimental DDT run-up distance (X_{D}, m)
0.2	1	4	0.8	2	5
1	5	0.8	0.16	0.4	0.75
8	40	0.1	0.02	0.05	0.08

shock) generally propagates faster than the flame itself (see Fig. 3 and Table 2) resulting in an increase of the boundary layer thickness measured at flame positions along the tube, as shown qualitatively by the curve $\delta(x)$ in Fig. 9e.

To have a firmer ground in discussing the boundary layer, which was not actually registered in the tests, we took shadow photos of the boundary layer ahead of an accelerated flame in a number of separate tests. The tests were made in a square channel with the channel height and width equal to 50 mm. Stoichiometric hydrogen–oxygen mixtures at initial pressures below 1 bar were used. A sequence of the photographs showing the growth of the boundary layer with flame propagation is shown in Fig. 10. The lead shock was formed ahead of the flame, but it cannot be seen in Fig. 10, because it was far to the right outside the optical window. These photographs support the qualitative picture presented in Fig. 9.

A detailed evaluation of the thickness of the boundary layer at flame positions along the tube would require an appropriate solution for the flow ahead of the accelerated flame. The history of flame acceleration, mutual positions of the lead shock and the flame, and the flow speed, as a function of distance and time, would be required for such a detailed evaluation. At the same time, a simpler approximate solution can be suggested.

According to the classical theory of the turbulent boundary layer, its thickness does not depend significantly on the flow speed. If a constant speed flow along a wall with roughness d is considered, the boundary layer thickness, δ, is defined by the following two equations with logarithmic accuracy (see, e.g., Landau and Lifshitz [27]):

$$\frac{V}{v*} = \frac{1}{\kappa} \ln\left(\frac{\delta}{d}\right) + K \tag{3}$$

$$\delta = C \frac{x v*}{V} \tag{4}$$

where V is the flow speed; $v*$ is a turbulent pulsation velocity in the boundary layer; κ, K, and C are constants; x is the distance along the flow. The ratio $V/v*$ can be eliminated from these equations and the thickness of the boundary layer will then be just a function of distance, x. This function is close to linear and engineering formulas are available [28], such as:

$$\frac{\delta}{x} = \text{constant} \left(\frac{x}{d}\right)^{-1/7} \tag{5}$$

We should note that in cases the tube roughness, d, is smaller than the thickness of the viscous sub-layer, $d_v = \nu/v*$ (ν is viscous diffusivity), the value of d_v instead of d should be used in Eqs. (3) and (5). This would result in a weak dependence of the boundary layer thickness on the flow speed (it is, however, not applicable for the conditions of the present tests, where $d \gg d_v$ for all the initial pressures).

The ratio x/V in Eq. (4) serves as a characteristic interaction time of the flow with the wall. The boundary layer grows with time during this interaction. Having this in mind, one can apply this theory to the situation of the boundary layer ahead of the flame. The interaction time, which determines the thickness of the boundary layer (Fig. 9), would be defined by a characteristic speed equal to the difference between the lead shock and the flame speeds. This characteristic value is close to the flow speed V, and because δ does not depend on the flow speed, Eqs. (3) and (4) can be used with their accuracy to estimate the function $\delta(x)$ in the situation shown in Fig. 9e.

In more rigorous terms, an application of Eqs. (3) and (4) for determination of $\delta(x)$ function shown in Fig. 9e assumes that the flame travels in the middle point between the lead shock and the ignition point. This is a reasonable assumption for estimates with the accuracy of a factor of 2 (see, e.g., Fig. 3 and Table 2). To give some more credit to such a simple model, we should notice that the flame position itself is not well defined, because of its complicated shape (see, e.g., Fig. 10). Also the thickness of the boundary layer itself is not well defined either. The value of δ, thus, should rather be considered as a characteristic scale of turbulent pulsations near the flame brush.

For the range of initial pressures between 4 and 8 bar, the run-up distances determined in the present tests were from 2.5 to 1.3 times the tube radius. Under these conditions, the fresh gas flow prior to the onset of detonation is essentially three dimensional. The growth of the boundary layer cannot

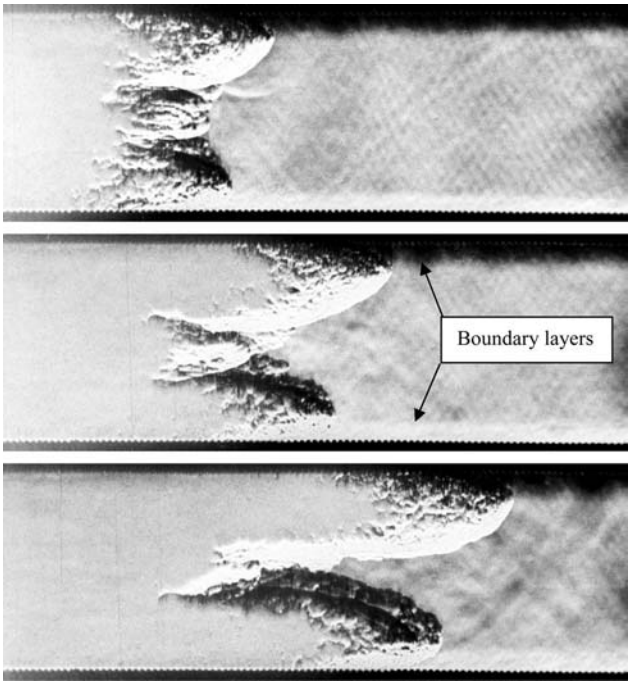

Fig. 10 Sequence of shadow photographs (0.1 ms between frames) showing boundary layers ahead of accelerated flame. Flame propagates from left to right; speed of lead flame edges is about 320 m/s. Boundary layers are seen as dark regions on the top wall and as lighter regions in the bottom wall of the channel. Wall roughness is 1 mm; mixture is stoichiometric H_2–O_2 at initial pressure of 0.6 bar

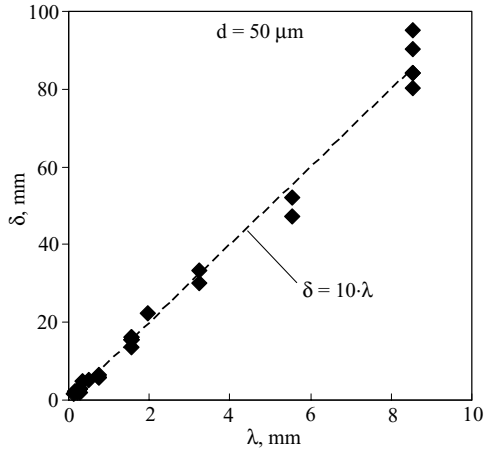

Fig. 11 Scale of turbulent pulsations (boundary layer thickness) at DDT locations

be illustrated by the qualitative picture presented in Fig. 9 and the model described in this section is not directly applicable.

5.3 Scale of turbulent pulsations at DDT location

Using the model described in the previous section, one can estimate the scale of turbulent pulsations at the run-up distance (substituting x with X_D in Eq. (4)). These turbulent motions are mostly related to the boundary layer generated by the flow ahead of the flame brush. A comparison of the scale of these pulsations (or boundary layer thickness) at locations where the onset of detonation was observed with the detonation cell width is presented in Fig. 11. The empirical constants in Eqs. (3) and (4) were taken to be: $\kappa = 0.4$; $K = 5.5$; and $C = 0.3\sqrt{2}$ as suggested by Landau and Lifshitz [27]. It is seen that for all the initial pressures the value of δ is 1 order of magnitude larger than λ with a rather good accuracy:

$$\delta(X_D) \approx 10\lambda. \tag{6}$$

Although for initial pressure from 4 to 8 bar the model for the boundary layer thickness is not directly applicable, the high-pressure data correlate well in Fig. 11. Some explanations for this behavior can be suggested. It may be argued that the gas flow ahead of the flame is also formed under these initial conditions. Despite of generally three-dimensional flow pattern, this flow is parallel to the wall at locations close to it. Equations (3) and (4) may be applicable with their accuracy to this situation. Because the flame position is not clearly defined in this case, one can define the maximum boundary layer thickness for the time of transition, replacing the characteristic interaction time x/V in Eq. (4) with t_D. This would assume that the value of V in Eq. (4) is given by the ratio X_D/t_D, while the value of V in Eq. (3) is essentially the flow speed. It is interesting to note that X_D/t_D is about 300 m/s, what is very close to the flow speed. Thus, application of this model for high-pressure data gives an estimate of the maximum boundary layer thickness at the time of transition. This may be suggested as an explanation for a good correlation of the high-pressure data in Fig. 11. We should notice that this might not be the case for other mixtures or tubes.

The detonation cell size of the original mixture was used in the comparison shown in Fig. 11. The state of the mixture near the flame brush, however, is different due to the mixture pre-compression behind the lead shock. The lead shock can approximately be characterized by the following typical parameters determined from the data for initial pressure from 0.2 to 1 bar: Mach number $\sim$ 1.5; overpressure ratio $\sim$ 1.4; temperature ratio $\sim$ 0.32. The detonation cell sizes, λ, of the initial mixture state and that for the mixture state behind the shock, λ_{ps}, were compared using the model of Gavrikov et al. [18]. It showed that for the shock parameters presented earlier, the post-shock cell size is 1.5 times smaller than that in the initial mixture state with a very good accuracy over all the range of the initial pressures. Thus, the scaling with the local cell size gives the same order of magnitude, and the following relation can be suggested instead of Eq. (6):

$$\delta(X_D) \approx 15\lambda_{ps}. \tag{7}$$

This looks as a very reasonable result. Indeed, the scale of pulsations controls the characteristic nonuniformity size and the mixing scale, or the size of the detonation kernel that can trigger the onset of detonation. The latter was shown to be greater than λ by about 1 order of magnitude [24, 25, 26] for the onset of detonation to be possible. It is thus reasonable to suggest that the onset of detonation in the present tests was observed as soon as the scale of the turbulent pulsations, which were mostly connected with the boundary layer, increased during flame acceleration up to about 15 times the local detonation cell sizes λ_{ps} (or 10 times the detonation cell sizes of the initial mixture).

The results available are not sufficient to describe details of the onset of detonations in the tests. It is not clear where exactly the detonations were originated. One possibility is that the detonation kernels, or hot spots, were formed ahead of the flame brush due to numerous interactions of pressure waves and turbulent motions, as it was observed in numerical simulations [29, 30]. Another option is that the onset of detonations occurred within the flame brush and the mixing of combustion products and reactants played a key role in triggering the detonation. It can be argued that a certain minimum size of the detonation kernel should have been formed. In both these options, the scale of turbulent motions controls the size of the detonation kernels.

Taking the scale of the turbulent motions, δ, as an input, one can estimate, whether the intensity of turbulence is sufficient to break the laminar flamelets and to mix products and reactants faster than the reaction occur, or not. The maximum size of the mixed products/reactants pocket, Δ_m, can be estimated following the model presented in [4]. The

model defines the mixed pocket as an eddy with turnover time, τ_v, which is shorter than characteristic chemical time, τ_c. The values of τ_v and τ_c are given by: $\tau_v = L_v/u'_v$; and $\tau_c = \delta_T/S_L$, where L_v is the eddy size and u'_v is the turbulent velocity at scale L_v. With assumption of the Kolmogorov turbulence, this yields:

$$\frac{\Delta_m}{\delta_T} = \left(\frac{\delta_T}{L_T}\right)^{1/2} \left(\frac{u'}{S_L}\right)^{3/2} \tag{8}$$

The integral scale of turbulence, L_T, is controlled by the scale of pulsations, δ, in our case. The turbulent velocity scale u' is defined by the flow speed $V \sim 300$ m/s. Taking into account that for the mixtures tested the laminar flame thickness satisfies, $\delta_T \approx \lambda/24$, Eqs. (6) and (8) give the required estimate:

$$\Delta_m \approx \delta/20. \tag{9}$$

This estimate suggests that efficient mixing of products and reactants would be only possible at scales of about 1 order of magnitude smaller than the integral turbulent scale, or boundary layer thickness. Thus, the option that the detonation kernel of a size comparable with the boundary layer thickness, δ, could be formed in the flame brush as a mixed pocket of reactants and products is not supported by this estimate.

5.4 Model predictions

It may be suggested that the link between the scale of turbulent motions (boundary layer thickness) and the detonation cell size (Eq. (6)) is useful for estimations of the run-up distances to DDT in various tubes and mixtures. Although the data of the present study alone are not sufficient to prove the generality of the correlation given by Eq. (6), some interesting predictions can be suggested.

According to the present results, the onset of detonations in relatively smooth tubes occurs when the maximum boundary layer thickness ahead of the flame grows up to about 10λ. Since this maximum thickness is expected to grow nearly linear with the flame propagation distance, the run-up distance to DDT appeared to be proportional to the cell size ($X_D/\lambda \approx 550$ in our case) and independent of the tube diameter. The coefficient of proportionality is expected to decrease with the tube wall roughness, d, or more rigorously with $\ln(d)$.

The model to estimate the run-up distances and interpretation of the experimental results presented here may be only valid for tubes with diameter $D \gg \lambda$. In particular, if D is less or about 20λ (depending on tube roughness), the turbulent boundary layer prior to the onset of detonation may occupy all the tube cross section. In this case, the scale of turbulent pulsations will be influenced by the tube diameter, D, and the run-up distance will depend on D. Thus, for relatively insensitive mixtures, a growth of the run-up distance with the tube diameter can be expected as observed in some of the earlier studies. One should be also cautious, if the model predicts that transition to detonation may occur at distances comparable to tube diameter (roughly, for $D > 200\lambda$), because of possible importance of three-dimensional effects. Although the results of present tests show good correlation with D/λ up to 600, this might not be the case for other mixtures or tubes.

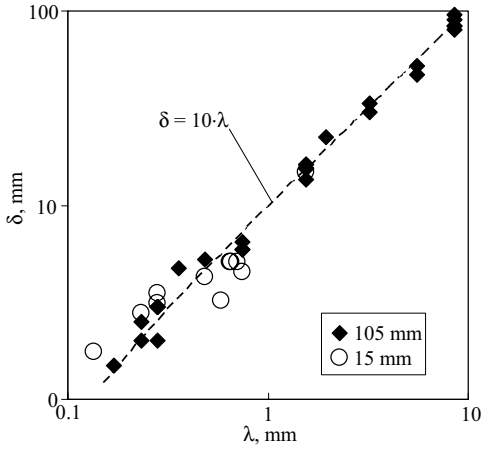

Fig. 12 Comparison of boundary layer thickness at DDT locations in two different tubes

Independence of the run-up distance on the tube diameter (at constant d) for relatively sensitive mixtures ($D > 20\lambda$) is a remarkable prediction, which can be evaluated against available experimental data. Recently, a series of tests with DDT in stoichiometric hydrogen–oxygen mixtures were performed in a tube with the internal diameter of 15 mm and wall roughness of 10 μm [31]. Although the main focus of tests [31] was different, the run-up distances were extracted from the experimental data for the range of initial pressures from 1 to 10 bar. The run-up distances observed in 15-mm tube were close to those in 105-mm tube for the same initial pressures. The maximum thickness of boundary layer at DDT location for these two tubes is shown in Fig. 12. Since most of the tests in [31] (2003) were with $\lambda < 1$ mm, the plot in Fig. 12 is given in logarithmic scale as different from Fig. 11. It is seen that the correlation is rather good within the accuracy of the model presented here.

6 Conclusions

We have presented results of experimental study on run-up distances to DDT in a smooth 105-mm tube filled with sensitive mixtures having detonation cell sizes up to 3 orders of magnitude smaller than the tube diameter. Stoichiometric hydrogen–oxygen mixtures were used in the tests with initial pressure ranging from 0.2 to 8 bar. The dependence of the run-up distance on the initial pressure was found to be close to the inverse proportionality. Experimental pressure

records showed that a compression wave with a lead shock was formed ahead of the flame at a certain stage of the flame acceleration process.

It was suggested that the flow ahead of the flame results in formation of the turbulent boundary layer. This boundary layer plays an important role in the flame acceleration and controls the scale of turbulent motions in the flow. A simple model was suggested to estimate the maximum scale of the turbulent pulsations (boundary layer thickness) at flame positions along the tube with an accuracy of about a factor of 2. The scale of turbulent motions controls the characteristic nonuniformity size, or the size of pre-conditioned regions of mixture that can trigger the onset of detonation. The latter was previously shown to be greater than λ by 1 order of magnitude [24, 25, 26] for detonation onset to be possible.

The onset of detonation in the present tests was observed as soon as the scale of the turbulent pulsations, δ, increased during flame acceleration up to about 15 times the local detonation cell size λ_{ps}, or about 10 times the cell size of the initial mixture. It is remarkable that this observation is shown to be valid over a wide range of the detonation cell widths from 0.1 to 10 mm within the limits of accuracy of the cell size data.

The model for approximate evaluation of the maximum size of turbulent motions, δ, during flame acceleration and the correlation with detonation cell size, $\delta \approx 10\lambda$, gives a basis for estimation of the run-up distances to DDT in relatively smooth tubes. This approach can only be applied for very sensitive mixtures or for sufficiently large tube diameters: $\delta < D/2$ (roughly, $D > 20\lambda$). One should be also cautious, if the model predicts that transition to detonation may occur at distances comparable to tube diameter (roughly, for $D > 200\lambda$), because of possible importance of three-dimensional effects. A comparison with the data obtained in a 15-mm tube was found to be in accord with the model presented. Other fuels should be also tested to check the universality of the results presented here.

Acknowledgements The authors would like to thank Prof. J. Shepherd, Prof. A. Khokhlov, and Dr. A. Kuhl for helpful discussions at 19th ICDERS in Hakone. The work was supported by Forschungszentrum Karlsruhe.

References

1. Urtiew, P., Oppenheim, A.K.: Experimental observations of the transition to detonation in an explosive gas. Proc. R. Soc. Lond. Ser. A **295**, 13–28 (1966)
2. Lee, J.H., Knystautas, R., Chan, C.K.: Turbulent flame propagation in obstacle-filled tubes. In: Proceedings of the 20th Symposium (International) on Combustion, pp. 1663–1672. The Combustion Institute, Pittsburgh, PA (1984)
3. Peraldi, O., Knystautas, R., Lee, J.H.: Criteria for transition to detonation in tubes. In: Proceedings of the 21st Symposium (International) on Combustion, pp. 1629–1637. The Combustion Institute, Pittsburgh (1986)
4. Dorofeev, S.B., Kuznetsov, M.S., Alekseev, V.I., Efimenko, A.A., Breitung, W.: Evaluation of limits for effective flame acceleration in hydrogen mixtures. J. Loss Prev. Process. Ind. **14**, 583–589 (2001)
5. Veser, A., Breitung, W., Dorofeev, S.B.: Run-up distances to supersonic flames in obstacle-laden tubes. J. Phys. IV Fr. **12**, 333–340 (2002)
6. Schelkin, K.I.: Occurance of detonation in gases in rough-walled tubes. Soviet J. Tech. Phys. **17**(5), 613 (1947)
7. Soloukhin, R.I.: Deflagration to detonation transition in gases. Soviet Prikladn. Mech. i Techn. Phys. (Appl. Mech. Techn. Phys.) (4), 128 (1961)
8. Lafitte, P., Dumanois, P.: Compt. Rend. Acad. Sci. Paris **183**, 284 (1926)
9. Lafitte, P.: Influence of temperature on the formation of explosive waves. Compt. Rend. Acad. Sci., Paris **186**, 951 (1928)
10. Egerton, A., Gates, S.F.: Proc. R. Soc. Lond. Ser. A **114**, 152 (1927)
11. Egerton, A., Gates, S.F.: Proc. R. Soc. Lond. Ser. A **116**, 516 (1927)
12. Schelkin, K.I., Sokolik, A.S.: Soviet. Zhurn. Phys. Chem. **10**, 479 (1937)
13. Campbell, G.A., Rutledge, P.V.: Detonation of hydrogen peroxide vapour. Inst. Chem. Eng. Symp. Ser. 33, Institute of Chemical Engineering, p. 37. London (1972)
14. Bollinger, L.E., Fong, M.C., Edse, R.: Experimental measurements and theoretical analysis of detonation induction distance. Am. Rocket Soc. J. **31**, 588 (1961)
15. Bollinger, L.E., Laughrey, J.A., Edse, R.: Experimental detonation velocities and induction distances in hydrogen–nitrous oxide mixture. Am. Rocket Soc. J. **32**, 81 (1962)
16. Salamandra, G.D., Bazhenova, T.V., Zaicev, S.G., Soloukhin, R.I.: Some methods for investigation of fast-running processes. Acad. Nauk SSSR, Moscow (1963)
17. Manzhalei, V.I., Mitrofanov, V.V., Subbotin, V.A.: Measurement of inhomogeneities of a detonation front in gas mixtures at elevated pressures. Combust. Explos. Shock Waves (USSR) **10**, 89–95 (1974)
18. Gavrikov, A.I., Efimenko, A.A., Dorofeev, S.B.: Detonation cell size predictions from detailed chemical kinetic calculations. Combust. Flame **120**, 19–33 (2000)
19. Reynolds, W.C.: The Element Potential Method for Chemical Equilibrium Analysis: Implementation in the Interactive Program STANJAN Version 3. Department of Mechanical Engineering, Stanford University, Palo Alto, California (1986)
20. Gavrikov, A.I., Bezmelnitsyn, A.V., Leliakin, A.L., Dorofeev, S.B.: Extraction of basic flame properties from laminar flame speed calculations. In: Proceedings of the 18th International Colloquium on the Dynamics of Explosions and Reactive Systems, ISBN #0-9711740-0-8, University of Washington, July, 2001, pp. 114/1–114/5 (2001)
21. Koroll, G.W., Kumar, R.K., Bowles, E.M.: Burning velocities of hydrogen–air mixtures. Combust. Flame **94**, 330–340 (1993)
22. Zel'dovich, Ya.B., Librovich, V.B., Makhviladze, G.M., Sivashinsky, G.I.: On the development of detonation in a non-uniformly preheated gas. Astronautica Acta **15**, 313–321 (1970)
23. Lee, J.H.S., Knystautas, R., Yoshikawa, N.: Photochemical initiation and gaseous detonations. Acta Astronautica **5**, 971–972 (1978)
24. Dorofeev, S.B., Efimenko, A.A., Kochurko, A.S., Chaivanov, B.B.: Evaluation of the hydrogen explosions hazard. Nucl. Eng. Design **148**, 305 (1994)
25. Khokhlov, A.M., Oran, E.S., Wheeler, J.C.: A theory of deflagration-to-detonation transition in unconfined flames. Combust. Flame **108**, 503–517 (1997)
26. Dorofeev, S.B., Sidorov, V.P., Kuznetsov, M.S., Matsukov, I.D., Alekseev, V.I.: Effect of scale on the onset of detonations. Shock Waves **10**, 137–149 (2000)

27. Landau, L.D., Lifshitz, E.M.: Hydrodynamics, 3rd edn., p. 736. Nauka, Moscow (1986)
28. Loiciansky, L.G.: Mechanics of Fluid and Gas, 5 edn., p. 736. Nauka, Moscow (1978)
29. Khokhlov, A.M., Oran, E.S., Thomas, G.O.: Numerical simulation of detonation initiation in a flame brush: the role of hot spots. Combust. Flame **119**, 400–416 (1999)
30. Khokhlov, A.M., Gameso, V.N., Oran, E.S.: Effects of boundary layers on shock-flame interactions and DDT. In: Proceedings of the 18th International Colloquium on the Dynamics of Explosions and Reactive Systems, July, 2001, University of Washington, ISBN #0-9711740-0-8 (2001)
31. Kuznetsov, M., Singh, R.K., Breitung, W., Stern, G., Grune, J., Friedrich, A., Sempert, K., Veser, A.: Evaluation of structural integrity of typical DN15 tubes under detonation loads. Report Forschungszentrum Karlsruhe, December (2003)